3D Flow measurement using particle tracking velocimetry (PTV) in porous media

Mohammad Amin Kazemi[1], Reza Sabbagh[2], Lisa Kinsale[1], Hirad Soltani[1], and David S. Nobes*,[1]

[1]Applied Thermofluids Lab., University of Alberta, Department of Mechanical Engineering, Edmonton, Canada

[2]RGL Reservoir Management Inc., Calgary, Canada

* david.nobes@ualberta.ca

Abstract

This paper presents a particle tracking velocimetry (PTV) system for measuring the flow within a porous medium at pore scales. Refractive index matching allows full optical access to the inner pores of the porous medium. By analyzing the images taken from a single camera, the in-plane components of the velocity at different locations in the depth were obtained from the PTV algorithm. By assuming the concept of continuity of an incompressible liquid, the gradients of the in-plane components were used to calculate the out-of-plane component of the velocity in each plane. The approach developed here has the potential to be implemented in measuring the flow field in any other application to obtain the out-of-plane component of the velocity.

1 Introduction

The flow of a liquid within a porous medium appears in some applications such as flow in biological tissues (Khaled and Vafai, 2003), ground water resources (Ryan and Elimelech, 1996), oil reservoirs (Peter *et al.*, 2010), membrane and filters (Vafayi, 2011), to name a few. Understanding the details of flow in a porous medium is a key step in better understanding and optimization of porous systems. Porous media are typically investigated as a bulk without interrogating details of the flow in individual pores. In applications such as steam assisted gravity drainage (SAGD) oil production and the subsurface flow of ground water, it is essential to explore the flow behavior at pore scales. This is important information when considering different systems failure mechanisms such the clogging of pores by fine particles in the region around the oil production well and to predict the movement of chemical contaminants in soils during the subsurface flow of ground water.

Studying the flow at subpore dimensions however, has many challenges. Limits in the measurement devices, range of applications, spatial and time resolutions are some of these issues (Werth *et al.*, 2010). Due to the difficulties and limitations of the measurement techniques, experimental observations of the flow field at subpore scales are scarce in the literature. To quantify the fluid velocity within the pores, optical measurements such as Laser Doppler Velocimetry (LDV) and Particle Image/Tracking Velocimetry (PIV/PTV) have been utilized in the past. However, optical measurements are limited as most porous media samples are not transparent which makes the measurement zone optically inaccessible. Refractive index matching (RIM) between the carrier fluid and the porous medium is one of the methods to overcome this problem. By matching the refractive indices of the model material and the fluid, the entire system becomes transparent which enables the optical probing of the tracer particles in the flow. Although flow measurement in porous media can be undertaken using confocal imaging (Cavazzini, 2012) and refractive index matching, most of the research in this field has been devoted to the two dimensional (2D) flow measurement or

visualization in simplified geometries. This has limited the investigations to structured porous media where the light can pass through the medium with no refraction. However, most real porous media such as biological tissues and geological formations are formed randomly in which the flow behavior is more complex and has a three dimensional (3D) nature.

In the present work, the flow through an unstructured porous medium (randomly packed glass spheres) is investigated to obtain the three components of the velocity over a three dimensional region (3C3D) at the pore scale. For this purpose, we have employed a shadowgraphic particle tracking velocimetry (SPTV) approach in a refractive index-matched medium. This paper describes the theoretical framework undertaking this type of study, the experimental setup for capturing and processing of data into full 3C3D measurements of the flow field. Although our motivation has been to analyze the 3D flow within a porous medium, the approach can be implemented in any other relevant field.

2 Experimental methods and procedures

In plane components (x,y) of velocity (u,v) can be captured using a standard planar PTV algorithm. The out of plane (z) position of the measurement can be defined by the position of the focal plane and its resolution by the depth of focus. By illuminating the entire test cell and scanning a thin focal plane over the depth of the porous medium, images of the tracer particles at several depth of the volume can be collected. The out-of-plane component of the velocity (w) in each layer is then calculated from continuity of an incompressible liquid, as:

$$\frac{\partial u}{\partial x}+\frac{\partial v}{\partial y}+\frac{\partial w}{\partial z}=0 \qquad (1)$$

where u, v and w are velocity components, x and y are the in-plane coordinates, and z is the out-of-plane coordinate. Figure 1 shows how the continuity equation can be used to calculate w from the in plane components u and v. By performing a planar PTV for each layer in the volume the in-plane components of the velocity (u,v) and subsequently the velocity gradients, $\partial u/\partial x$ and $\partial v/\partial y$ are obtained. The variation of the third velocity component in the depth, $\partial w/\partial z$ can be then calculated from Eq. 1. Finally, the values of w in each plane are determined from a linear extrapolation between the closest solid wall and the point of interest (Kazemi, Elliott and Nobes, 2016) assuming that the velocity components (including the out of plane component, w) at the solid walls are zero.

$$w=\left(\frac{\partial w}{\partial z}\right)\Big|_{dz} dz \qquad (2)$$

where dz is the distance between the point of interest and the solid wall.

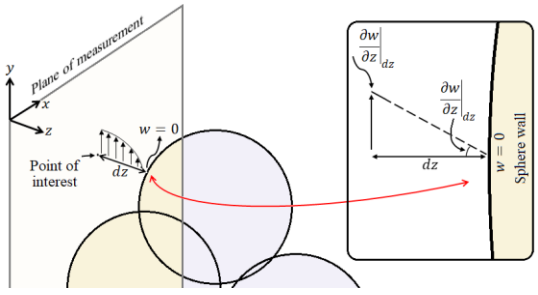

Figure 1 Application of the continuity equation to compute the third component of the velocity from the in-plane components.

The experimental setup utilized to quantify the flow field within the porous medium is demonstrated in Figure 2. The setup consisted of a flow channel which was designed using a commercial laser cutter (VersaLaser VLD Version 3.50; Universal Laser Systems). The flow cell had a 5.8 mm depth (Optix

Acrylic; Plaskolit Inc.) was confined with two PMMA side windows and randomly filled with many 1 mm borosilicate glass spheres to mimic the porous medium. The channel was mounted vertically and canola oil which was already mixed with 8 µm tracer particles (glass spheres) was infused into the channel by using a fluid delivery syringe pump ('11' Plus, Harvard Apparatus Inc.) at a rate of 15 ml/hr. The suspension was injected from the bottom of the channel, moved upward in the opposite direction of the gravity to exit the channel. To track the seeded particles in the flow, the flow cell was illuminated by an LED light source (BX0404, Advanced Illumination Inc.), and a CCD camera (CMOS SP - 5000M – PMCL, JAI Inc.) with a resolution of 2000 pixel × 1800 pixel recorded the images of seeded particles. The camera was equipped with an infinity corrected microscopic lens (Olympus Plan N 4x/0.10) and suitable optics (Infini Tube FM-200, Boulder, CO). The assembly of the lenses provided a field of view of 2.37mm × 2.13mm and a depth of field of ~ 0.08 mm. The image acquisition rate was controlled by using a function generator (AFG3021B, Tektronix Inc.) which was synched to the camera. Data sets of 500 sequential images were collected at a frequency of 25 Hz at each depth with an exposure time of 150 µs. To capture the images at different depths in the volume, the position of the flow cell with respect to the camera was changed manually using a fine pitch micrometer adjuster (148-801ST; Thorlabs) with a 10 µm graduated scale.

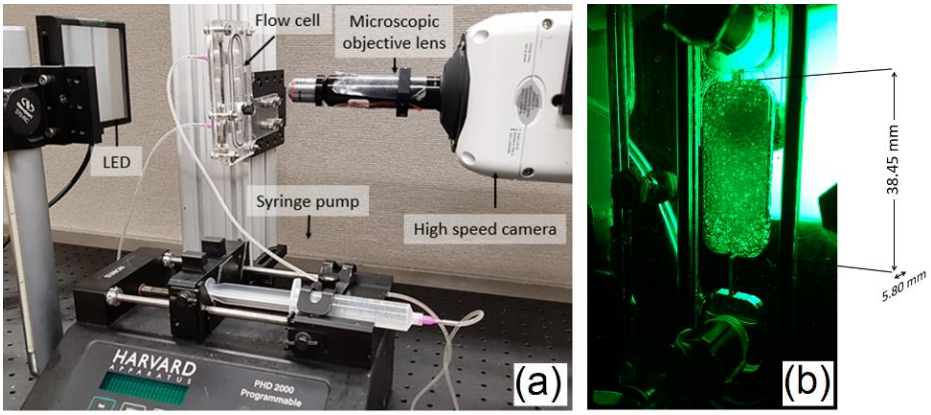

Figure 2 (a) Experimental setup and its components, (b) a magnified view of the flow channel, and (c) schematic representation of the flow channel and its dimensions. The packed bed is 38.45 mm high and 5.80 m deep.

3 Data analysis and velocity vector calculation

In the velocity vector calculation procedure, the unwanted out-of-focus particles should be eliminated from the images to attain a more precise velocity vector field. A great portion of the out of focus particles can be removed by a thresh-holding filter as their intensities are lower than those of the in focus particles. However, this does not always occur and sometimes the out of focus particles are included in the analysis after applying this filter(Benson and French, 2007) and will, on occasion, introduce errors in the velocity calculation. For instance, the maximum intensity of particle 1 shown in Figure 3(a) which is an in focus particle is 234 counts, while that of particle 2 which appears to be an out of focus particle is 254 counts. Thus, if a thresh-holding filter is used to remove the out of focus particles, regardless of the strength of the filter, particle 2 always remains longer than particle 1 in the processed image and results in producing erroneous velocity vectors (outliers). As an alternative method to avoid this problem, the local standard deviation for each pixel was calculated by considering the 3-by-3 pixels in the neighbor around the corresponding pixel as shown in Figure 3(b). This parameter is large for the pixels that have a remarkable contrast with their neighbors. As it can be seen in Figure 3(b), the more a particle is in focus, the brighter the circle surrounding the particle is. Applying this filter following by subtracting a certain value from the values of local standard deviation removes almost all of the out of focus particles while identifies the in focus ones which are shown in Figure 3(c). It should be noted that in Figure 3(c), the open circles were filled by using a bandwidth filter to make them ready for performing a PTV algorithm.

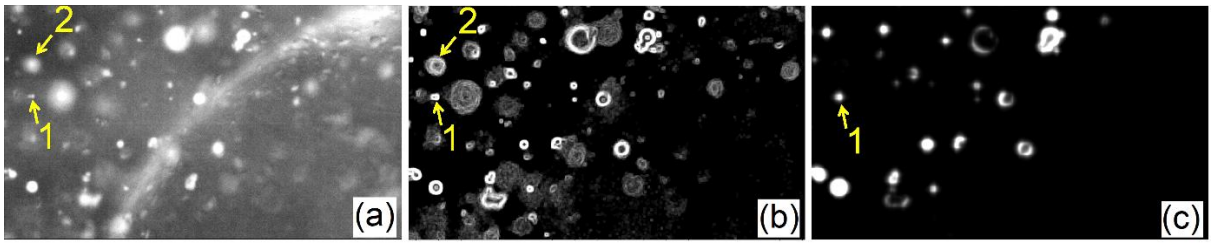

Figure 3 The process of removing the out of focus particles from the collected images and making them ready for performing PTV algorithm. (a) Inverted raw image, (b) local standard deviation of the images, and (c) the empty circles are filled using a Bandwidth filter. Some intermediate steps of image preprocessing such as subtracting the minimum of 500 images from all original images to filter out the constant noise, or the amplification of the intensities after subtracting a certain value from the intensities to remove the noise are not shown here.

After preprocessing of the images, the PTV algorithm was applied. In this step, particles were detected based on a certain intensity threshold followed by detection of the local maxima within a kernel of 17 × 17 pixel^2. A band-passed filter was applied to the detected particles to accept only particles with a diameter within the range of 3–30 pixels. The location of each particle was determined with a Gaussian sub-pixel fit estimator. The particles were allowed to be tracked over 2 frames. The data was filtered by limiting the magnitude of the displacement of particles to be smaller than 14 pixels in the horizontal direction (x) and 15 pixels in the vertical direction (y). The maximum displacement gradient allowed in the vector field was set to 0.07 pixel/pixel as suggested to be the maximum valid value (Keane and Adrian, 1992). Since the raw velocity data obtained from the PTV were sparse and randomly distributed across the image plane, the velocity in the empty pixels were estimated using a two dimensional cubic interpolation algorithm (MATLAB R2017b, The MathWorks Inc.).

4 Results and discussion

The in-plane velocity components obtained from the 2D PTV processing discussed earlier are shown in Figure 4. The different panels in Figure 4 show the velocity field at different depths of the porous medium, with the panel (a) being the closest to the front wall of the test cell.

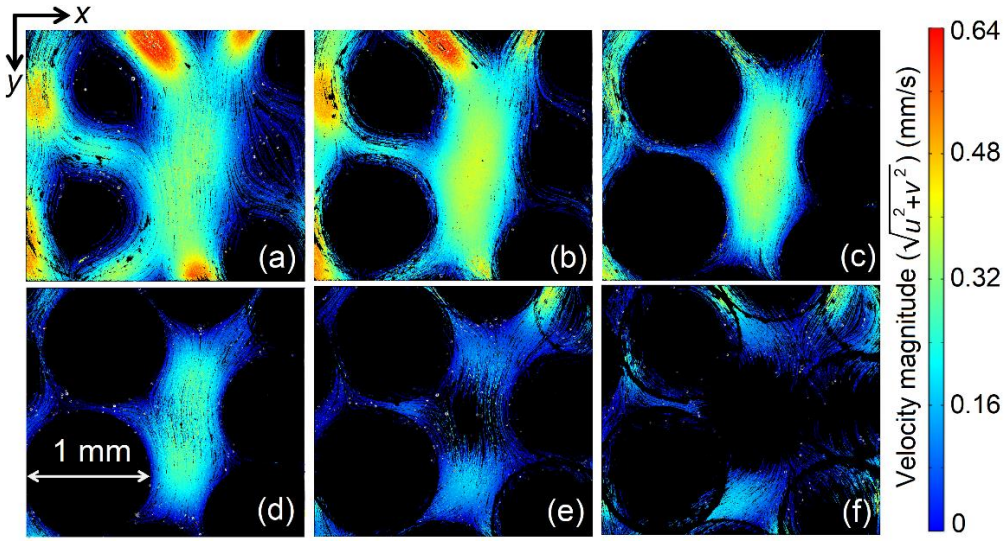

Figure 4 Two dimensional representation of the in-plane velocity components at different depth of the porous medium obtained from PTV. Panels (a) – (f) are located at z = 0.24 mm, z = 0.34 mm, z = 0.44 mm, z = 0.54 mm, z = 0.64 mm, z = 0.74 mm respectively. The front wall is assumed to be at z = 0.

The liquid suspension flows upward in the direction opposite to that of gravity. As it can be seen in Figure 4, the liquid accelerates in the narrower regions satisfying the continuity equation (Eq. 1). By comparing Figure 4 (a) – (f), it seems that the magnitude of the in-plane velocity vectors ($\sqrt{u^2+v^2}$) diminishes by the distance from the front wall that is located at $z = 0$. This implies that the liquid flows faster near the wall compared to the central region of the porous medium which can be due to the smaller resistance against the flow near the side walls. The out-of-plane component of velocity (w) at different planes was computed from the continuity equation (Eq. 1). As w calculated from this approach strongly depends on the gradients of the in-plane velocities ($\partial u/\partial x$, $\partial v/\partial y$) rather than the velocities (u,v) themselves (see to Eq. 1), the in-plane velocities (u,v) need to be smoothed before being introduced into Eq. 1 to get a coherent w from the continuity equation. Figure 5 (a) and (b) show a comparison between the smoothed velocity profiles and the non-smoothed ones obtained from PTV. Smoothing was performed using a 2D smoothing function (Greg Reeves, 2009). As Figure 5 (a) and (b) show, the smoothing algorithm captures a consistent pattern in the velocity data sets and eliminates the outliers which cause a sharp variation in the gradients of the velocity. By using the smoothed gradients, $\partial w/\partial z$ (from Eq. 1) and subsequently w (from Eq. 2) were calculated which are illustrated in Figure 6.

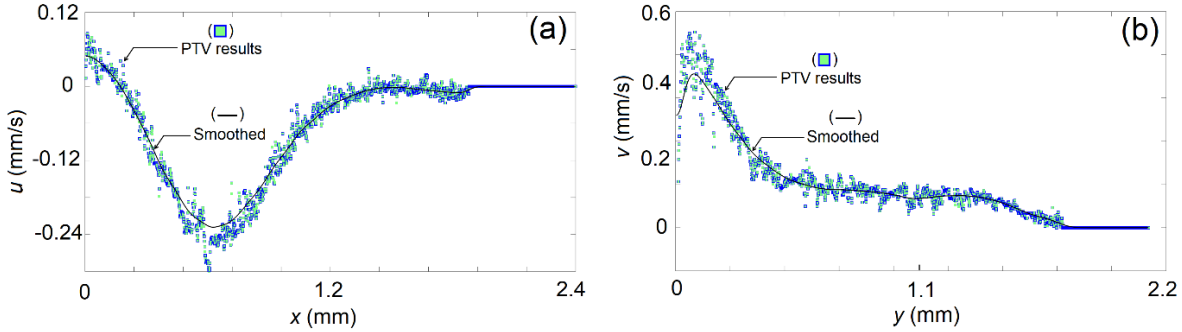

Figure 5 Smoothing the in-plane velocity data obtained from PTV in order to calculate the out-of-plane component of velocity.

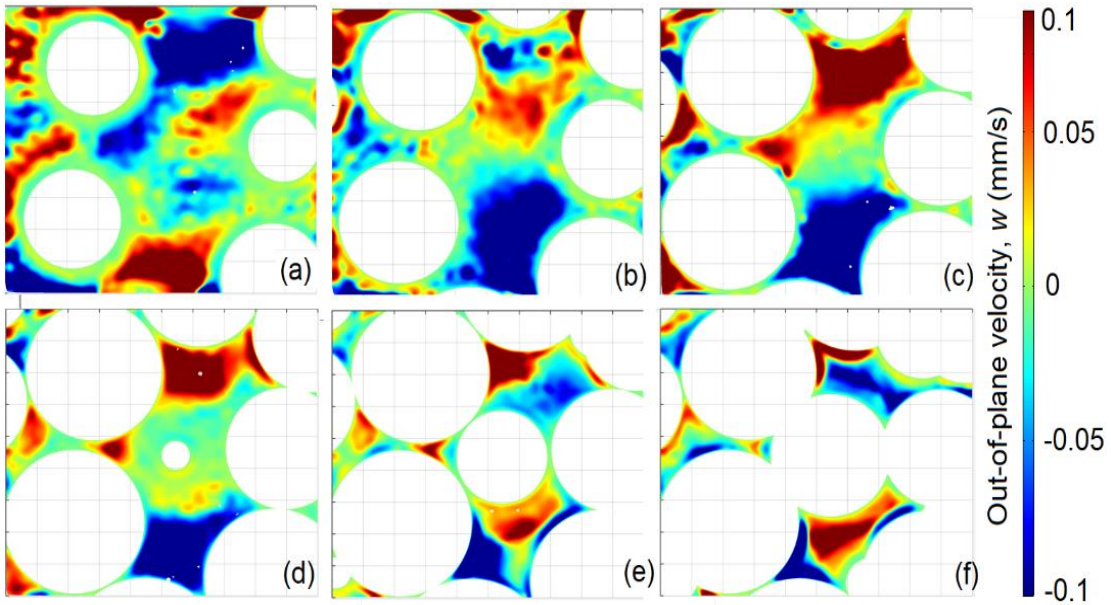

Figure 6 The out-of-plane velocity component, w, calculated from the continuity equation (Eq. 1). Panels (a) – (f) are located at $z = 0.24$ mm, $z = 0.34$ mm, $z = 0.44$ mm, $z = 0.54$ mm, $z = 0.64$ mm, $z = 0.74$ mm respectively. The front wall is assumed to be at $z = 0$. The z axis is normal to the planes and positive downward.

5 Conclusion

The 3D flow of oil through a packed bed of spherical glass particles was investigated at pore scale using a particle tracking velocimetry technique. To gain optical access to the volume of the medium, refractive index matching was utilized. The in-plane velocity components at different depths of the porous medium were obtained by the time tracking of the individual particles in the flow. To obtain the out-of-plain component of velocity, the continuity equation was employed. An improvement to the velocity calculation would be achieved if a thinner depth of focus was used. The use of the continuity equation combined with the result of 2D PTV showed promising, although preliminary, results to determine the full velocity measurements in the volume using only a single camera, and has a great potential to be employed in other applications where implementation of the 3D velocimetry measurements is difficult. However, this approach needs to be further explored and developed in the future by comparing it to the results from other existing approaches such as tomographic PIV and defocusing PTV.

Acknowledgements

The authors gratefully acknowledge financial support from Natural Sciences and Engineering Research Council (NSERC) of Canada, the Alberta Ingenuity Fund, and the Canadian Foundation for Innovation (CFI), and RGL Reservoir Management Inc.

References

Benson, T. and French, J. R. (2007) 'InSiPID: A new low-cost instrument for in situ particle size measurements in estuarine and coastal waters', *Journal of Sea Research*, 58(3), pp. 167–188. doi: 10.1016/j.seares.2007.04.003.

Cavazzini, G. (2012) *The particle image velocimetry – characteristics , limits and possible applications*. Rijeka, Croatia: InTech.

Greg Reeves (2009) 'smooth2a function v. 1.0 MATLAB file exchange, https://www.mathworks.com/matlabcentral/fileexchange/23287-smooth2a'.

Kazemi, M. A., Elliott, J. A. W. and Nobes, D. S. (2016) 'Determination of the three components of velocity in an evaporating liquid from scanning PIV', in *The 18th International symposium on the application of laser and imaging techniques to fluid mechanics, Lisbon Portugal, July 4 – 7*. Lisbon Portugal.

Keane, R. D. and Adrian, R. J. (1992) 'Theory of cross-correlation analysis of PIV images', *Applied Scientific Research*, 49(3), pp. 191–215. doi: 10.1007/BF00384623.

Khaled, A.-R. A. and Vafai, K. (2003) 'The role of porous media in modeling flow and heat transfer in biological tissues', *International Journal of Heat and Mass Transfer*, 46(26), pp. 4989–5003. doi: 10.1016/S0017-9310(03)00301-6.

Peter, G. *et al.* (2010) 'Characterizing Flow in Oil Reservoir Rock Using Smooth Citation Accessed Characterizing Flow in Oil Reservoir Rock Using Smooth Particle Hydrodynamics', *AIP Conference proceedings*, pp. 278–283.

Ryan, J. N. and Elimelech, M. (1996) 'Colloid mobilization and transport in groundwater', *Colloids and Surfaces A: Physicochemical and Engineering Aspects*, 107(95), pp. 1–56. doi: 10.1016/0927-7757(95)03384-X.

Vafayi, K. (2011) *Porous media; Applications in biological systems and biotechnology*, *CRC Press*. Taylor & Francis Group.

Werth, C. J. *et al.* (2010) 'A review of non-invasive imaging methods and applications in contaminant hydrogeology research', *Journal of Contaminant Hydrology*. Elsevier B.V., 113(1–4), pp. 1–24. doi: 10.1016/j.jconhyd.2010.01.001.